JGR Biogeosciences

RESEARCH ARTICLE
10.1029/2024JG008011

Droughts Amplify Soil Moisture Losses in Burned Forests of Southeastern Amazonia

Antônio C. Silveiro[1,2], Divino V. Silvério[1,3], Marcia N. Macedo[2,4], Michael T. Coe[2,4], Leandro Maracahipes[2,5,6], Maria Uribe[6], Leonardo Maracahipes-Santos[2], Paulo Tarso S. Oliveira[7], Ludmila Rattis[2,4], and Paulo M. Brando[1,2,4,6]

[1]Universidade do Estado de Mato Grosso (UNEMAT), Programa de Pós-Graduação em Ecologia e Conservação, Nova Xavantina, Brazil, [2]Instituto de Pesquisa Ambiental da Amazônia (IPAM), Canarana, Brazil, [3]Universidade Federal Rural da Amazônia (UFRA), Capitão Poço, Brazil, [4]Woodwell Climate Research Center (Woodwell Climate), Falmouth, MA, USA, [5]Universidade Estadual de Campinas (Unicamp), Campinas, Brazil, [6]Yale School of the Environment, Yale University, New Haven, CT, USA, [7]Universidade Federal de Mato Grosso do Sul (UFMS), Campo Grande, Brazil

Key Points:

- During the driest months of the year, burned forests showed significant reductions in soil moisture compared with unburned forests
- The drought event of 2015/2016 caused greater reductions in soil moisture in the burned forest than in the unburned forest
- Both burned and unburned forests increased water use throughout the 8-m soil column from 2011 to 2018

Supporting Information:

Supporting Information may be found in the online version of this article.

Correspondence to:

A. C. Silveiro,
acsilveiro@gmail.com

Citation:

Silveiro, A. C., Silvério, D. V., Macedo, M. N., Coe, M. T., Maracahipes, L., Uribe, M., et al. (2024). Droughts amplify soil moisture losses in burned forests of southeastern Amazonia. *Journal of Geophysical Research: Biogeosciences*, *129*, e2024JG008011. https://doi.org/10.1029/2024JG008011

Received 18 JAN 2024
Accepted 28 SEP 2024

Abstract Soil moisture is a crucial variable mediating soil-vegetation-atmosphere water exchange. As climate and land use change, the increased frequency and intensity of extreme weather events and disturbances will likely alter feedbacks between ecosystem functions and soil moisture. In this study, we evaluated how extreme drought (2015/2016) and postfire vegetation regrowth affected the seasonality of soil water content (0–8 m depth) in a transitional forest in southeastern Amazonia. The experiment included three treatment plots: an unburned Control, an area burned every three years (B3yr), and an area burned annually (B1yr) between 2004 and 2010. We hypothesized that (a) soil moisture at B1yr and B3yr would be higher than the Control in the first years postfire due to lower transpiration rates, but differences between burned plots would decrease as postfire vegetation regrew; (b) during drought years, the soil water deficit in the dry season would be significantly greater in all plots as plants responded to greater evaporative demand; and (c) postfire recovery in the burned plots would cause an increase in evapotranspiration over time, especially in the topsoil. Contrary to the first expectation, the burned plots had lower volumetric water content than the Control plot. However, we found that droughts significantly reduced soil moisture in all plots compared to non-drought years (15.6%), and this effect was amplified in the burned plots (19%). Our results indicate that, while compounding disturbances such as wildfires and extreme droughts alter forest dynamics, deep soil moisture is an essential water source for vegetation recovery.

Plain Language Summary As extreme droughts and wildfires have become more common in southeastern Amazonia, they could alter soil moisture availability, but the intensity of these compounding effects still needs to be understood. This study investigates the impact of the extreme drought of 2015/2016, postfire vegetation recovery, the return of water to the atmosphere, and their interacting effects on water distribution across the soil profile in three treatment plots: an unburned Control, an area burned every three years, and an area burned annually from 2004 to 2010. Contrary to expectations, we found that soil moisture in the burned plots decreased in the years following the last experimental fire (2010), even as the vegetation recovered. Drought events significantly reduced soil moisture across all plots, but this effect was amplified in the burned plots. As land use changes increase and climate change intensifies, such drought-induced soil drying may become more common, exacerbating the impacts of wildfires on ecosystem resilience and forest health across much of the region.

1. Introduction

Amazon forests maintain high evapotranspiration rates, contributing to regional cooling and rainfall throughout the year by taking up water from deep soil layers. In the southeastern Amazon, up to 50% of regional rainfall has been attributed to forest water recycling (Aragão, 2012; Lovejoy & Nobre, 2018; Marengo & Espinoza, 2015; Salati et al., 1979; Spracklen et al., 2012; Staal et al., 2018). In extreme cases, the roots of Amazonian trees may reach depths greater than 10 m, providing access to large soil water stores for evapotranspiration (ET) (Nepstad et al., 1994). Despite the importance of this forest climatic function for biodiversity, carbon cycling, and economic activities (e.g., food and energy production), there is growing evidence that forest degradation associated with human disturbances is decreasing the capacity of the system to cycle water (Nobre et al., 2016; Wright

et al., 2017). Extreme weather events (e.g., heatwaves and droughts) superimposed on human activities may further contribute to ET reduction, especially in the southeast Amazon (Coe et al., 2017; Silvério et al., 2015). Central to Brazil's recent agricultural production, this region is also where droughts have become increasingly common (Brando et al., 2013).

Weakening the hydrological cycle can jeopardize both forests and agricultural production by triggering important changes in the regional climate of the southern Amazon. Droughts often cause extreme reductions in soil water storage and increased air dryness, as represented by vapor pressure deficit (VPD) (Solander et al., 2020). Although many Amazonian tree species have adaptations to cope with seasonal soil water stress and high air temperatures, these adaptations often involve reducing transpiration rates to prevent damage to hydrological systems (Brando, 2018; Giardina et al., 2018; McDowell et al., 2020; Nepstad et al., 2007; Pfautsch, 2016; Pittermann, 2010). Despite these strategies, many tree species have experienced increased mortality rates during severe droughts, as reported in 2005 (Phillips et al., 2009), 2010 (Lewis et al., 2011), and 2015/2016 (Aragão et al., 2018). Changes in ET that occur as trees regulate water losses or experience excess mortality during these events strongly influence soil moisture, making ET a key indicator of ecosystem stress and recovery after disturbances.

Plant adaptations to cope with Amazon droughts often cause increased forest flammability. Tree physiological responses to drought promote fuel accumulation on the forest floor (i.e., litter, branches, and dead trees) and increased air dryness in the forest understory (Aragão et al., 2018; Brando et al., 2014; De Farias et al., 2017; Sungmin et al., 2020). In the presence of human ignition sources, surface fires can affect large tracts of these flammable forests. During the 2000s, more than 85,000 km^2 of primary forests were burned in southern Amazonia (Morton et al., 2013), mainly during the droughts of 2005, 2007, and 2010 (Brando, Paolucci, et al., 2019). Because forest fires drastically reduce canopy cover, burned forests are expected to evapotranspire less (Brando, Silvério, et al., 2019), especially where fires are most intense (e.g., during droughts and along forest edges). However, it remains unclear whether reductions in forest ET are proportional to leaf area index (LAI) in burned forests, given that complex interactions between postfire forest recovery and weather variability could either promote or dampen ET. A study in southeast Amazonia showed that ET quickly recovered after severe degradation by fire, edge effects, and a windthrow event (Brando, Silvério, et al., 2019; Brando, Paolucci, et al., 2019). Similarly, Miller et al. (2011) found that changes in forest energy balance (including ET) caused by logging were minor and short-lived.

The El Niño–Southern Oscillation (ENSO) event refers to changes in atmosphere–sea interactions due to changes in sea surface temperatures (SST) in the eastern tropical Pacific Ocean. Abnormally warm ocean temperatures in this region are known as El Niño (warm mode), whereas abnormally cold temperatures are known as La Niña (cold mode) (Solander et al., 2020; Trenberth, 1997). The 2015/16 ENSO was one of the most intense events in recorded history (L'Heureux et al., 2017), causing widespread drought and reductions in soil moisture throughout the Amazon (Solander et al., 2020), yet its impacts on human-disturbed forests are unclear. The drier edges of the transitional forests between Amazonia and the Cerrado were expected to experience more intense water stress, yet it is unclear whether the 2015–2016 drought altered soil moisture in deeper soil layers and whether it affected primary and degraded forests similarly. Here, we quantified soil water dynamics in a forest degraded by prescribed fires, a blowdown event in 2012, and multiple drought events (Figure 1). We took advantage of long-term measurements of soil water (from 0.3 to 8.0 m) in a transitional forest (2011–2018) along the ecotone between Amazonia and the Cerrado. We hypothesized that (a) burned plots with lower LAI would have higher soil moisture in the years immediately following fire and blowdown events, compared to the unburned Control, but differences between these forests would decrease over time as degraded forests recovered (Figure 1a); (b) the extreme drought of 2015–2016 would cause unusual soil moisture reductions, and this effect would be amplified in burned plots due to increased transpiration by rapidly growing early succession species; and (c) postfire recovery in the burned plots would cause an increase in ET over time, mainly in the topsoil.

Our goal was to evaluate how changes in vegetation cover affect soil moisture (Hypothesis 1) in experimental plots burned between 2004 and 2010. Furthermore, we aimed to analyze whether the 2015–2016 extreme drought affected soil moisture and whether this effect was greater in burned plots (Hypothesis 2) compared with an unburned Control. Finally, we assessed whether evapotranspiration (estimated by soil moisture) was highest in the burned plots, especially in the topsoil (Hypothesis 3). The transitional forests of the southeastern Amazon are in a drier region that is susceptible to forest fires. Understanding how burned forests alter soil moisture and how

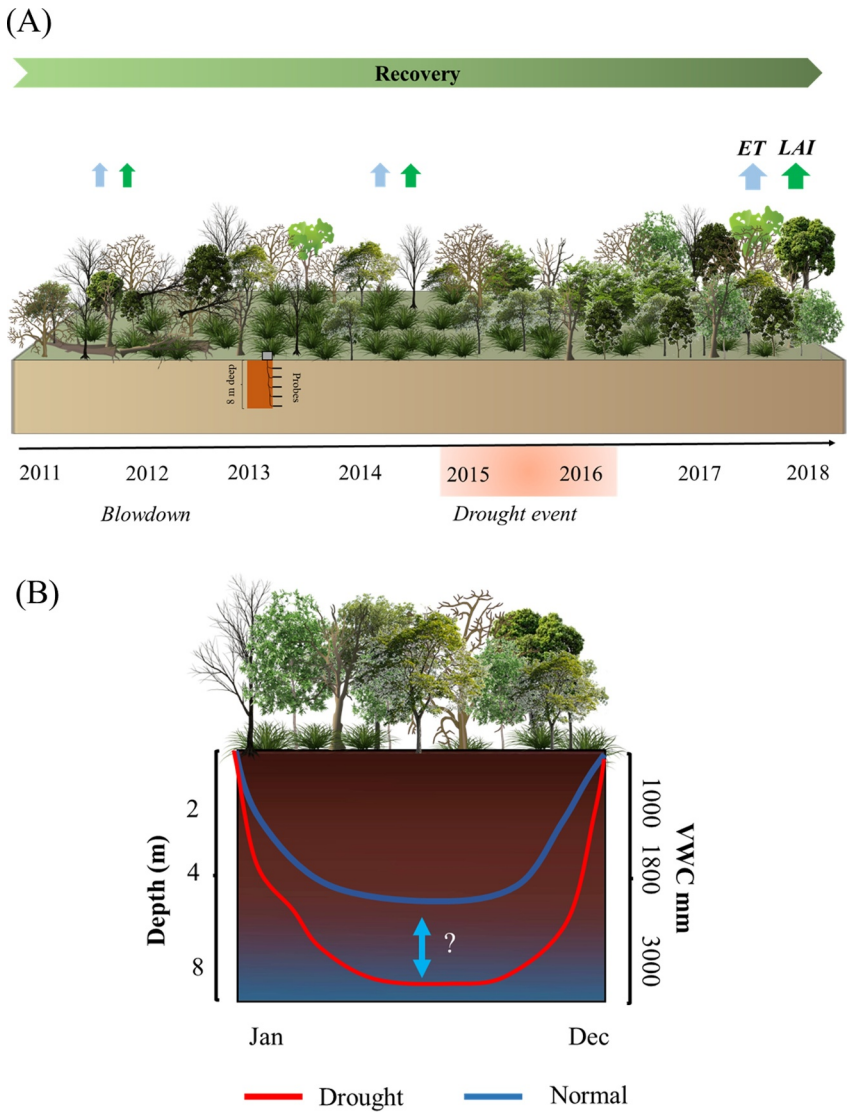

Figure 1. Panel (a) Hypothetical diagram illustrating postfire recovery (LAI) and evapotranspiration (ET) with possible impacts on soil moisture (Hypothesis 1). Panel (b) Uncertainties about drought impacts on deep soil water storage and the intensity of reduction in volumetric water content in burned forests (Hypothesis 2).

extreme drought events can further reduce available soil water provides valuable information about the potential for recovery of this degraded vegetation and the likelihood that forests will remain intact in the region. To achieve these objectives, we used a unique and uninterrupted (2011–2018) time series of surface soil moisture up to 8 m deep in the Amazon–Cerrado transitional region.

2. Material and Methods

2.1. Study Site

The study was conducted at Tanguro Field Station (Fazenda Tanguro: Figure 2; −52.37683 and −13.07448), located on a private farm in the municipality of Querência in Mato Grosso state, Brazil. The farm encompasses ∼80,000 ha, with nearly 60% of the area covered by transitional forests along the ecotone between the Amazon (forest) and Cerrado (savanna) biomes. The forest canopy averages 20 m high (Balch et al., 2008; Nagy et al., 2015).

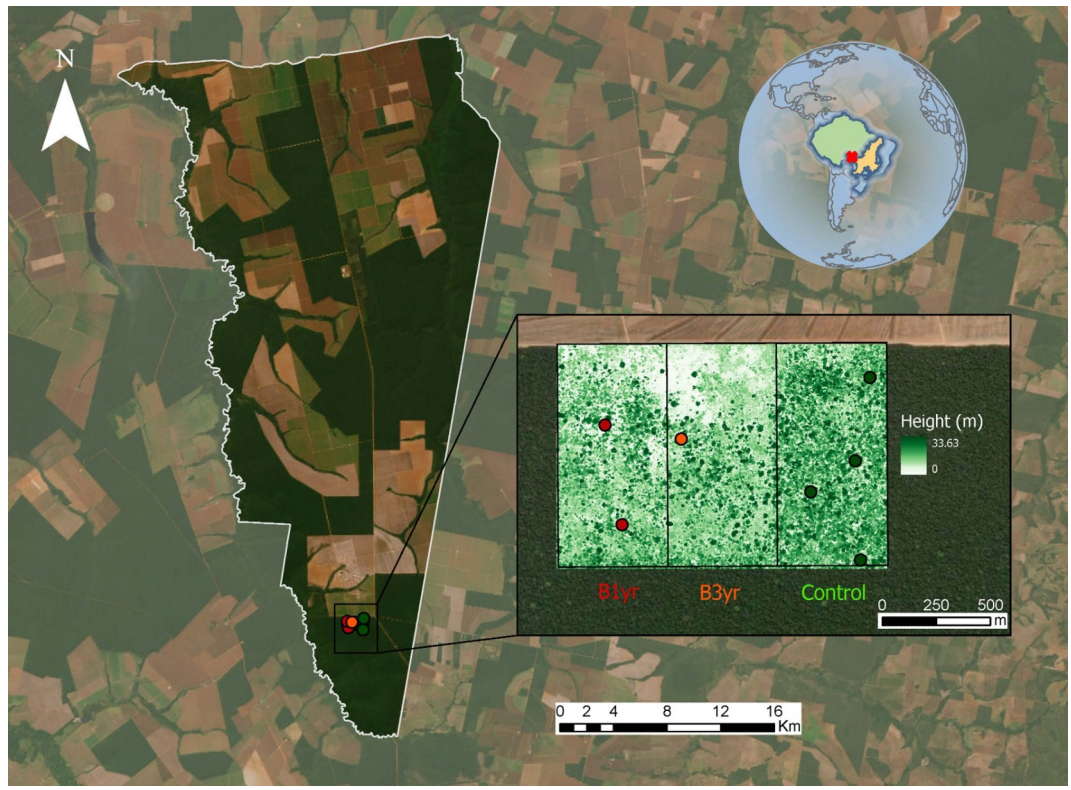

Figure 2. The forest plots and their location relative to the Brazilian Amazon region and the Xingu River basin (bottom left panel). The main panel (left) shows the location of Fazenda Tanguro. The green scale in the three plots (right) refers to the vegetation height obtained by Lidar in 2018. Within the plots, the geometric figures show the location of 8-m soil pits equipped with time domain reflectometry sensors. Colors indicate the locations of the soil pits in the plot burned every year (orange circle), the plot burned every 3 years (yellow circle), and the unburned Control plot (green circles).

According to the Köppen climate classification system, the climate in this area is Aw ("A" stands for tropical zone and "w" denotes a region with a dry winter). That is, our study site occurs in a tropical region with a dry winter (Alvares et al., 2013), with a dry season centered on the austral winter (April through September) and a hot, rainy season during the austral summer (October through March). Between 2011 and 2018, the majority of rainfall (80%–97%) in our study area occurred during the rainy season, according to local observations recorded by our meteorological station. The average annual temperature for the region ranges from 23 to 25°C, while the annual precipitation ranges from 1,700 to 2,200 mm (Alvares et al., 2013). The elevation varies between 299 and 403 m (mean 354 m), and the mean slope is 1.13° across the entire Fazenda Tanguro. The soils are predominantly Latosols and can reach up to 15 m in depth without physical impediments (Balch et al., 2008). Soil bulk density varies between 1.63 and 1.19 g/cm^3 for the three plots, being denser in the deep soil, while its granulometry is more clayey, mainly in the deep soil (from 3 m deep; see Figure S1 in Supporting Information S1).

2.2. Experimental Design

The study was conducted at the site of a long-term prescribed fire experiment spanning 150 ha (1,500 × 1,000 m; Figure 2). The experiment was divided into three subplots of 50 ha each, with three contrasting treatments: unburned plot (Control), triennial burning (B3yr, years: 2004, 2007, and 2010), and annual burning (B1yr, years: 2004 to 2010, except 2008), as described by Brando et al. (2014). The experiment was bordered by a deforested field with exotic grasses for cattle until 2008, when the pasture was converted to a soybean and corn field (Balch et al., 2008).

2.3. Data Collection and Analysis

2.3.1. Soil Moisture

We calculated soil moisture in 8-m soil pits installed in the Burned and Control plots, using the Time Domain Reflectometry (TDR) method (Topp et al., 1980). In each pit, we placed 11 sensors at depths from 0 to 8 m, spaced as follows: 0.0 m (surface), 0.3 m, and 0.5 m, followed by 1 m intervals until 8 m. The number of pits installed varied over time and between treatments. TDR systems were installed in two pits at the beginning of sampling (2010), one in the Control and the other in the B1yr plot. In 2011, we added two more pits in the Control and one in B1yr and B3yr plots. One of the pits in the Control collapsed in 2015 and was replaced the following year (Brando, Silvério, et al., 2019; Brando, Paolucci, et al., 2019). Until 2018, we measured soil moisture in six pits, three in the Control plot and three in the burned plots (two in B1yr and one in B3yr).

In the first 0.3 m of the soil profile, pairs of probes were arranged vertically (perpendicular to the surface). In contrast, at the other depths (between 0.5 and 8 m), the probes were inserted horizontally (parallel to the surface) throughout the profile, extending 0.5 m into the walls of the soil pit. We built a calibration curve before the permanent installation of the probes, using soil characteristics at each depth (bulk density; Figure S1 in Supporting Information S1). Three soil samples were collected for gravimetric water content (GWC) and soil density–one sample on the wall surface and the other two at 0.15 and 0.30 m (perpendicular to the wall), making up part of the length where the probes were inserted. Using GWC and soil density, we calculated the volumetric water content (VWC) and later correlated it with permissiveness (dielectric constant) using linear regressions (see Figure S2 in Supporting Information S1). After installing the probes, we covered the walls of the soil pits with plastic to minimize the evaporation gradient along the soil profile (see pre-installation of probes, Figure S3 in Supporting Information S1). More information about these soil moisture data can be found in Silveiro et al. (2024).

2.3.2. Daily Evapotranspiration Estimation

We estimated evapotranspiration during dry periods, defined as >10 consecutive rainless days (usually from May to September), using soil moisture data from the TDR. We assumed that the change in soil moisture from one day to the next represents a proxy for the evapotranspiration rate during these dry periods. Because soil evaporation and stream baseflow represent a small fraction of the variation in soil moisture following extensive periods without rain (Davidson et al., 2011; Markewitz et al., 2010), most of the observed changes in soil moisture likely represent plant transpiration (Brando, Silvério, et al., 2019). Although more open canopies in the burned plots could lead to higher evaporation rates, we found evaporation rates in a nearby site (<2 km away) with bare soil to be negligible after 10 rainless days. To evaluate the maximum depth at which plants affect soil moisture, we divided the transpiration rate into three depths: 0–2, 0–4, and 0–8 m. To do this, we grouped measurements taken from 0 to 2 m depth (superficial layer), from 0 to 4 m (middle layer), and from 0 to 8 m (entire profile) and analyzed them independently.

2.3.3. Selection of Drought Years

To define the drought years between 2011 and 2018, we used the Maximum Climatological Water Deficit (MCWD) as an index (Aragão et al., 2007; Malhi et al., 2008), where MCWD was calculated based on the monthly Cumulative Water Deficit within each annual cycle (Aragão et al., 2007). The 2015/2016 interval showed the most significant deficit in atmospheric humidity during our study period, which is consistent with the strong El Niño (warm SST anomaly) registered early that year in the Amazon (Yang et al., 2018). As with other analyses, we defined the 2015/2016 drought based on the MCWD anomaly during the hydrological year, starting in October 2015 and ending in September 2016, which was influenced by the strong El Niño event in 2015.

2.3.4. Precipitation and Leaf Area Index (LAI)

We used LAI to characterize the vegetation structure around the TDR pits over time (2011–2016). We collected the LAI quarterly by treatment with two LAI-2200C Plant Canopy Analyzers (LI-COR Biosciences Inc, Lincoln) (Brando, Silvério, et al., 2019; Brando, Paolucci, et al., 2019). For comparison with the LAI around the pits, we also show the behavior of the LAI for the entire area of the experiment (B1yr, B3yr, and Control), dividing between the edge (up to 200 m) and the interior of the forest (2011–2017). Precipitation data were obtained from our meteorological station, which collects continuous data (2011–2018) and is close to the study site (Balch et al., 2008; Rocha et al., 2014).

2.3.5. Data Analysis

We used a linear mixed model (LMM) to compare the VWC between the three treatments in the postfire periods, the 2015/2016 drought event, and normal years (Hypothesis 1). For this analysis, we used data from the three driest months of the year (i.e., August, September, and October). The response variable was the VWC at 8-m depth (from 0 to 8 m) and two variables as predictors: (a) the plots (Control, B1yr, and B3yr) and (b) the three different periods (postfire periods, the 2015/2016 drought event, and normal years). We added months and individual pits (seven pits) as random effects to the model. We applied the Tukey-Krame test to compare VWC means between treatment plots and periods. To test our model assumptions, we checked the residuals to examine the normality and homogeneity of variance in our data (Figure S4 in Supporting Information S1). This analysis was performed using the lmer function of the "*lme4*" package (Bates et al., 2015) in R software (R Core Team, 2023).

To analyze the effects of drought on the three treatment plots (Hypothesis 2), we subtracted the VWC (considering the entire soil water column) in the non-drought years (2011, 2012, 2013, 2014, 2017, and 2018) from the drought year (2015/2016). We first obtained the daily average by adding the VWC of the entire soil water column (0.3–8 m). The average VWC was then subtracted from the maximum VWC over the entire profile (Equation 1). Finally, we subtracted the VWC measured during non-drought years from the VWC during the drought year (Equation 2). For both metrics, we bootstrapped 2000 observations and analyzed the differences with a 95% confidence interval. To assess evapotranspiration (Hypothesis 3), we divided the soil column as follows: 0–2 m, 0–4 m, and 0–8 m, and computed the lower and upper limits around the mean with 95% confidence. This division of the soil column was used to analyze the extent of the effect of evapotranspiration from the vegetation.

$$\text{vwc\_dif} = (\text{vwc}_{\text{daily}} - \max(\text{vwc}_{\text{daily}})) \quad (1)$$

$$\text{vwc\_final} = (\text{vwc}_{\text{dif\_non-drought}} - \text{vwc}_{\text{dif\_drought}}) \quad (2)$$

Where $\text{VWC}_{\text{daily}}$ refers to the average daily sum of the VWC at all measured depths (summarized at 6-hr time intervals); $\text{VWC}_{\text{dif\_non-drought}}$ represents the daily average values in non-drought years; and $\text{VWC}_{\text{dif\_drought}}$ represents the daily average values in the drought year.

Equation 1 gives the degree of drying and wetting of the soil per day. To obtain the drying and wetting values, we applied a linear regression analysis (equation = days ~ VWC anomaly) using a breakpoint analysis. The soil drying period occurs between the wettest and driest periods of the year, and the degree of soil wetting starts from the first recharge and reaches the wettest value, usually in the following year. Equation 2 gives the size of the impact of drought on VWC. We applied Equations 1 and 2 for the entire soil column and for each profile section divided by 2-m depth (0–2 m, 2–4 m, 4–6 m, and 6–8 m) and we show the results by days (supplementary material) and by months.

To evaluate the combined effect of drought and fire on soil moisture thresholds, we first calculated the minimum and maximum daily VWC values for each period from the surface to 8 m depth. Next, we summarized the VWC by burn treatment, drought years versus normal years, and soil depth. We used the sum of the differences between maximum and minimum VWC throughout the entire time series (Equation 3) as a proxy for plant-available water.

$$\text{VWC}_{\text{available}} = \sum_{\text{i=depth}} (\text{VWC}_{\text{max}} - \text{VWC}_{\text{min}}) \quad (3)$$

Where $_{\text{depth}}$ denotes the soil depth interval.

3. Results

3.1. Seasonal Patterns and Treatment Effects

Overall, soil moisture decreased during the dry season and increased during the rainy season across all study years (Figure 3). This clear seasonal pattern of soil moisture, especially from 0 to 2 m (Figures 4a–4c), roughly matched precipitation patterns (Figure 4d). Soil drying generally began in mid-April (end of the rainy season) in the shallower portions of the profile, reaching deeper levels (up to 8 m) by mid-May. In most years, soil recharge in

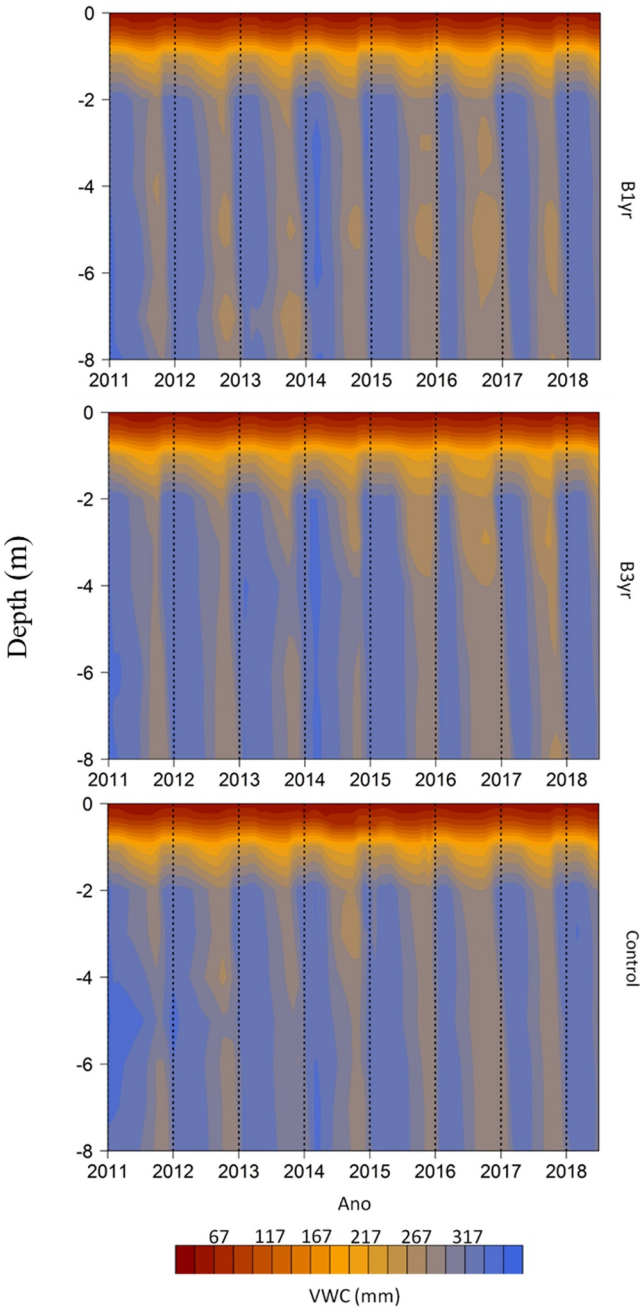

Figure 3. Volumetric water content in the soil profile (to 8 m deep) from 2011 to 2018 in each of three treatment plots: burned every year (*B1yr*), burned every three years (*B3yr*), and unburned (*Control*).

the first 2 m of the profile began in October (i.e., in the first month of the rainy season); however, deep soil moisture recharge during the drought of 2015–2016 took 2 months longer (i.e., beginning in December). In the rainfall recorded in our study area, 2015 was the driest year, ~900 mm below the historical average, whereas for the hydrological year 2015/2016, the difference from the historical average was −443 mm. The MCWD for the region (100-km buffer) in 2015/2016 was −427 mm compared to −425 mm in a non-drought year (from 2000 to 2018, except for 2007 and 2010 as they were two years of drought) (Caioni et al., 2020). The similarity of MCWD for the region is due to the low values for the years following droughts, such as 2011, 2012, and 2017.

3.2. Effect of Postfire on VWC

For the driest months of the year, our model showed significant differences between B1yr (other years) and Control plots (Figure 5; *p*-value: <0.01, *p*-value: <0.001). The VWC was ~100 mm (4%) higher for the Control than for the B1yr plot in both periods. On the other hand, there was no statistical difference between the Control plot and B3yr (*p*-value: 0.94, *p*-value: 0.46, *p*-value: 1.00, *p*-value: 0.94). Moreover, the postfire (2011/2012) period was generally wetter than other years (53 mm in B1yr and Control plots, and 38 mm in B3yr) but with no clear implications for the differences between plots. Fixed predictors of our LMM explained 30% of the variability of VWC data up to 8 m, whereas random effect predictors explained 40% (Figure 5). These patterns reinforce other results that emphasize the high seasonality of soil moisture throughout the year and a steeper reduction in soil moisture for burned plots.

3.3. Effects of the 2015/2016 Drought on VWC

During the ENSO event of 2015 and 2016, soil drying started in February—over two months earlier than usual (typically late April; Figure 6). From the wet-to-dry inflection point in February, it took ~235 days (~8 months, see Figure S5 in Supporting Information S1) for the soil profile to reach the lowest VWC values (relative to the maximum VWC) in the three experimental plots, corresponding to the an average water use of 2.5 mm/day (Figure S6 in Supporting Information S1) during the transition from wet to dry seasons. This differed significantly ($p = < 0.0001$) from non-drought years, when it took 202 days for VWC to reach minimum values (Table S1 in Supporting Information S1), with an average water use of 2.38 mm/day. After reaching its most negative value during the drought year (B1yr: −532.2 mm; B3yr: −545.8 mm; Control: −466.0 mm), soil moisture began to recover in mid-September, whereas in non-drought years (B1yr: −481 mm; B3yr: −430 mm; Control: −427 mm) recovery started in October. However, the total recovery of soil moisture was far greater in non-drought years than in the drought year (mean slope = 4.7 mm/day, p-value = < 0.0001). Our analysis by section of the profile showed that the topsoil (2 m) reached potential field capacity in non-drought years but not during the drought year (Figure S7 in Supporting Information S1).

The vegetation in our experimental burned plots accessed much of the water stored in the soil profile. The difference in VWC (0–8 m) between the minimum and maximum values of our time series averaged 607 mm (B1yr: 615 mm; B3yr: 654 mm; Control: 554 mm) (Figure 7), suggesting that the total volume of soil water available to plants was similar across the three treatments. However, in the Control, there was a detectable reduction in VWC in the deeper soil profile (between 2 and 4 m, and from 7 to 8 m) during the drought peak (Figure 7a). As a result,

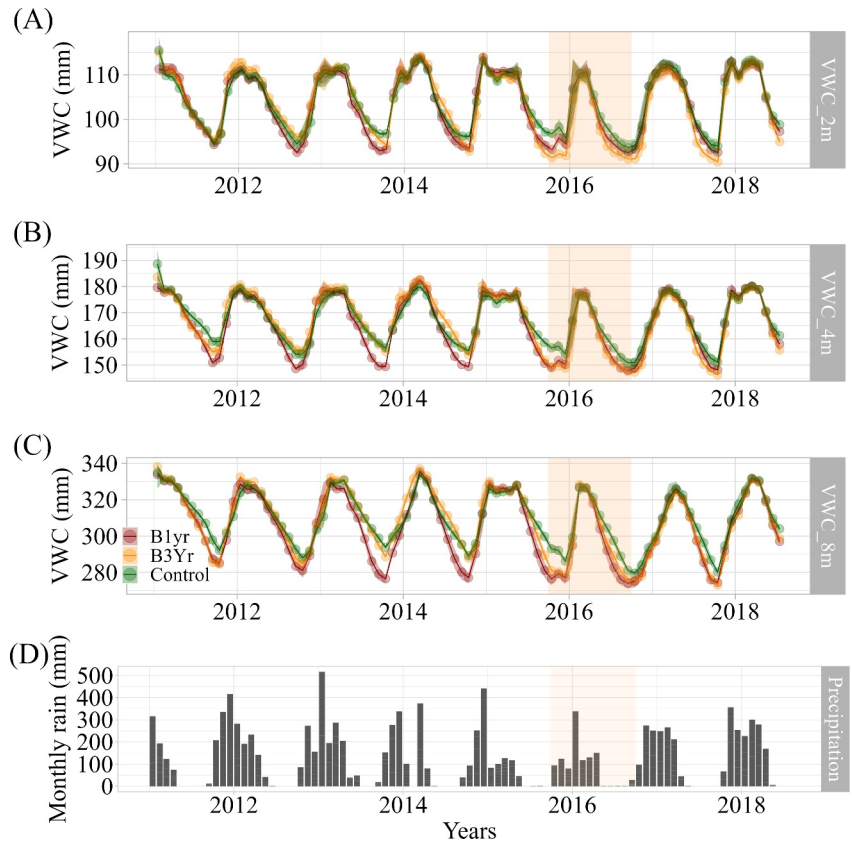

Figure 4. Monthly volumetric water content time series averaged to three different depths of the soil profile (Panel is 0–2 m, B is 0–4 m, and C is 0–8 m) for each fire plot: (*B1yr*—burned annually; *B3yr*—burned every 3 years; *Control*—unburned). Panel (d) shows monthly precipitation in our study area from 2011 to 2018. Orange shading indicates the drought of 2015/2016.

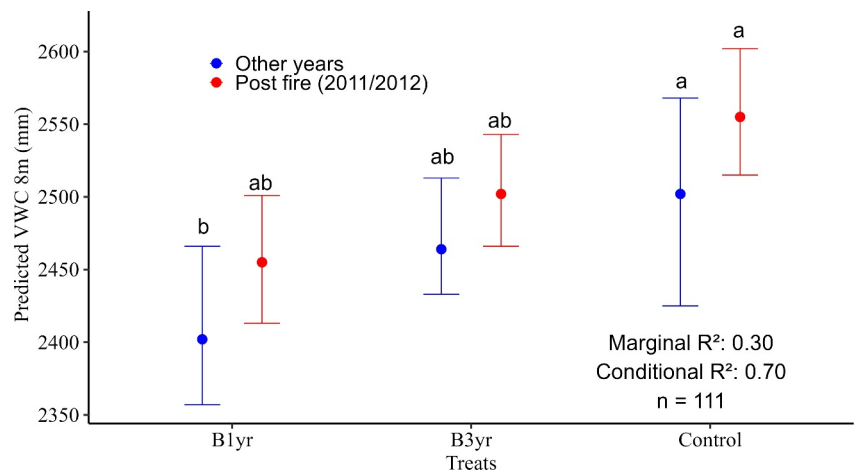

Figure 5. Predicted values of volumetric water content (VWC), based on a generalized linear mixed model of the influence of fire (Hypothesis 1). Different letters denote differences in VWC (0–8 m) between treatments (B1yr, B3yr, and Control) in post-fire and other years. We also tested for interaction between treatments, periods of postfire and other years.

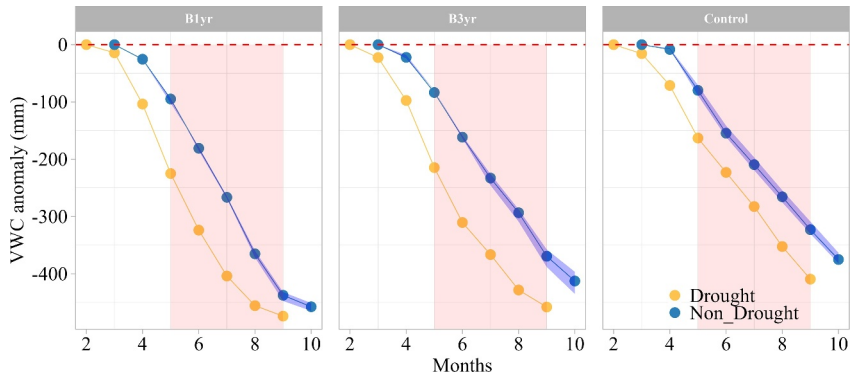

Figure 6. Variations in the soil water anomaly over the hydrological year. We calculated the difference between the average and maximum volumetric water content for each fire plot across the hydrological year. Pink shading denotes the dry season.

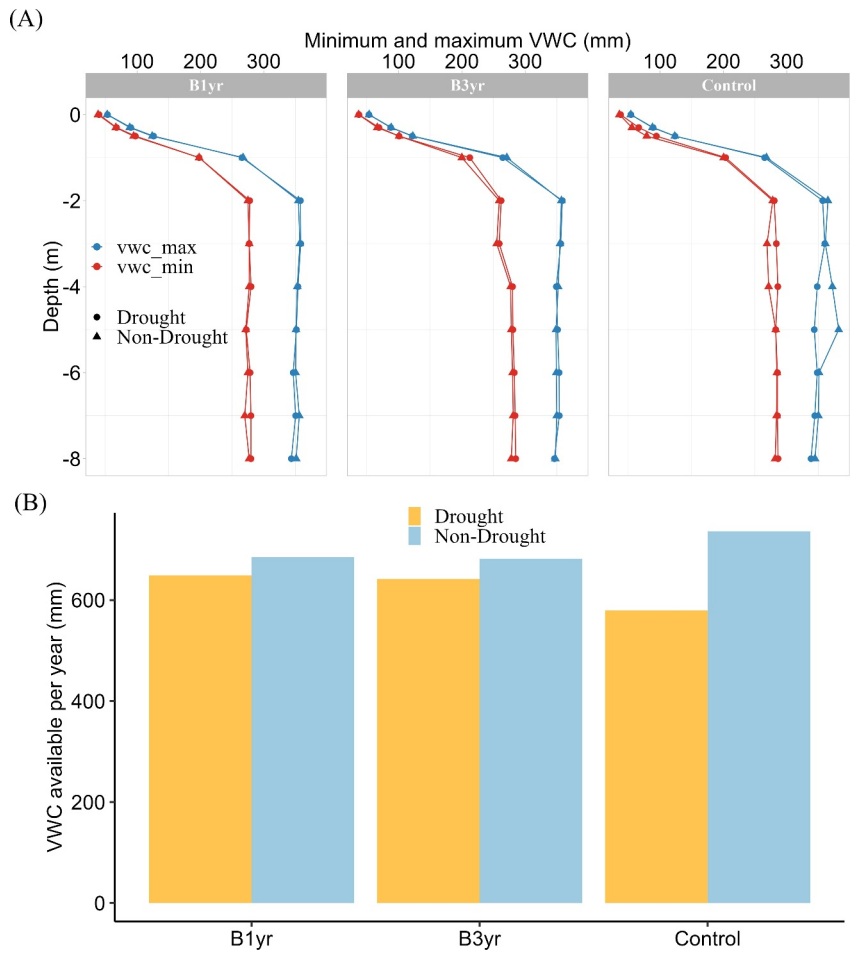

Figure 7. Soil moisture expressed as volumetric water content (VWC) was observed in 8-m soil pits within each burn plot. (a) Minimum and maximum VWC at each depth during the 2015/2016 drought (orange triangle), compared with all non-drought years (blue circle). (b) Estimated total water available to plants up to 8 m in drought and non-drought years.

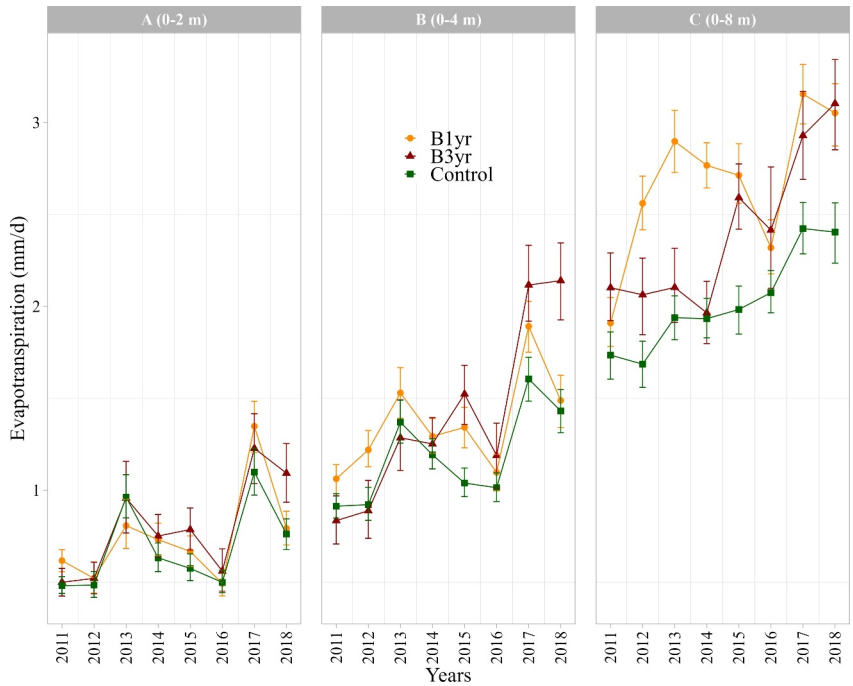

Figure 8. Average daily evapotranspiration (ET) in different subsections (0–2 m, 0–4 m, and 0–8 m) of the soil column in the three experimental plots. Bars around each mean indicate the 95% confidence interval. Note that panels (b, c) show cumulative ET from the soil surface down to the specified depth. Panel (b) thus represents the sum of total ET from 0 to 2 m panel (a) and total ET from 2 to 4 m, whereas panel (c) is the sum of panel (b) and the ET from 4 to 8 m.

in the Control plot, there was 17% (120 mm) less water available to plants during the drought year than in non-drought years, while for the burned plots, it was 6% (39 mm) for B3yr and 5% (36 mm) for B1yr.

3.4. Indirect Effect of Vegetation on VWC

Dry-season evapotranspiration was supported by plant water uptake throughout the entire soil profile (Figure 8). On average, the shallow portions of the soil profile (0–2 m) contributed 0.75 mm/day to dry-season ET (B1yr: 0.74 mm/day; B3yr: 0.80 mm/day; Control: 0.69 mm/day), which represented ∼22% of the total ET from 2011 to 2018 (Figure S8 in Supporting Information S1). The other three sections of the soil profile contributed similarly (2–4 m: 26%; 4–6 m: 26%; and 6–8 m: 25%) to dry season ET.

Considering soil water over the full 8 m profile reveals an average evapotranspiration rate of 3.31 mm/day (B1yr: 3.43 mm/day; B3yr: 3.48 mm/day; Control: 3.02 mm/day), which is consistent with average values previously reported for the region, especially if we discount from these values average baseflow for this site (range: from 0.6 to 0.9 mm; Hayhoe et al., 2011). Although the LAI was lower in the burned plots overall (Figure S9 in Supporting Information S1), evapotranspiration from 0 to 8 m was substantially higher at B3yr (17%) and B1yr (30%) compared to the Control from 2011 to 2018, even when differences in LAI between the Control and burned plots were more prominent (i.e., from 2011 to 2013, early in the postfire recovery compared to 2014 and 2018).

On an interannual scale, the highest daily ET generally occurred in 2017 (Figure 8c), except for B3yr, which showed an increase in ET in 2018. The observed decreases in ET (in all plots) during the 2016 drought were most pronounced in the topsoil (Figure 8a) and similar to those recorded earlier in the study period (2010 and 2011). The lowest evapotranspiration rates occurred in 2011 for B1yr and 2012 for the Control, two years with below-average annual precipitation that immediately followed the drought of 2010. For B3yr, the lowest evapotranspiration rates were observed in 2014. Moreover, we observed an interesting pattern in the deep soil (8 m), where daily evapotranspiration rates increased across all plots over time (39% for Control, 48% for B3yr, and 60% for B1yr), and drought-induced decreases were observed only in the burned plots.

4. Discussion

4.1. Effects of Post Fire and Drought on the Overall Soil Moisture Pattern

The clear seasonal pattern of drying and wetting (Figures 3 and 4) indicates the possible use of soil water by vegetation. This pattern is consistent with other studies carried out in the Amazon (Broedel et al., 2017; Jipp et al., 1998; Markewitz et al., 2010). However, unlike central (Broedel et al., 2017) and eastern Amazonia (Markewitz et al., 2010), the seasonality of deep soil moisture in our study area appears to be more intense (Figure 4c). Although this behavior may suggest root uptake throughout the soil profile (as shown in Figures 3 and 8), it may also be partly due to the high infiltration capacity of these soils and subsequent percolation (Scheffler et al., 2011).

We hypothesized that forest degradation in southern Amazonia would increase soil moisture (VWC) due to low ET during the early years of vegetation recovery, but this difference would decline as vegetation grew back. Contrary to our expectations, the Control plot exhibited a higher VWC than the burned plots (Figure 5), suggesting a greater use of soil water by the burned plot after the fire passed. The higher soil bulk density in plot B1yr compared with that in the Control plot (Figure S1 in Supporting Information S1) reinforces the idea of greater use of water by vegetation in the burned plots. This is corroborated by a sensitivity analysis (Figure S10 in Supporting Information S1), which indicates that the reduction in soil moisture would have been even greater if plot B1yr had the same soil density as the other plots. Furthermore, despite the lower canopy cover in the burned plots (Figure S9 in Supporting Information S1), postfire ET values were comparable to or higher than those in the Control plot, when considering the entire soil profile (Figure 8). Another explanation for these results may be related to the rapid postfire recovery of canopy cover in burned plots. As early successional species became more dominant, they likely demanded a higher ET per unit of LAI (Brando, Silvério, et al., 2019). Regardless of the mechanism, these findings highlight the critical role of recovering forests in re-establishing ET, an essential component of the hydrological cycle that affects precipitation patterns (Guillod et al., 2015; Spracklen et al., 2012; Staal et al., 2018) and triggers the earlier onset of wet season rains (Wright et al., 2017).

We also hypothesized that ET would increase as vegetation recovered over time. This hypothesis received strong support, given that ET increased faster in both burned plots than in the Control from 2010 to 2017 (Figure 7) (B3yr = 17%; B1yr = 30%). While this increase could be related to postfire recovery in the burned plots, the signal may be confounded by the increased evaporative demand associated with recent droughts, regional warming, and changing vegetation dynamics (Davidson et al., 2012). The increase in ET in 2017 and 2018, for example, may be a response to above-average rainfall following the unmet water demand during the 2015–2016 drought. Moreover, ET was more variable in the first 2 m than in the deeper soil layers, as seen in the years of more significant precipitation (2013 and 2017) and drought (2010, 2015, and 2016). Another important point was the reduction in evapotranspiration in 2016 that occurred in all plots, which may be related to the extreme drought conditions. During this period, there was a reduction in soil moisture up to 4 m in depth (Figures 8a and 8b). In 2011 and 2012, we also observed important reductions in ET, probably related to the 2010–2011 drought (Brando et al., 2014). This large variation in the upper layers may be associated with greater plant water use due to the higher density of fine-rooted biomass (Nepstad et al., 1994; Spanner et al., 2022). This behavior suggests that deep soil water contributes to more stable ET.

As predicted, the drought of 2015/2016 resulted in a stronger water deficit (e.g., MCWD: −427 mm) and a faster drop in VWC than in non-drought years for all experimental plots (Figure 6). We highlight two main points regarding the effects of this drought on VWC. First, soil drying started approximately 1 month before normal years and reached the lowest values over the entire time range (Table S1 in Supporting Information S1). Second, the difference in VWC between the dry and non-dry conditions was significant in the first 4 m as well as for the entire soil column (Figure S11 in Supporting Information S1). This result reinforces our conclusion that a combination of extreme drought events can jeopardize forest recovery from wildfires by increasing water stress. In addition, the absence of recharge of soil water (even in the first 2 m) in the year following an extreme drought event (Figures 4 and S7 in Supporting Information S1) suggests that surface soil depends on subsequent rainfall for recharge after drought events in the Amazon, which can take many months to occur.

Depletion of the VWC by drought also reduces evapotranspiration and contributes to a higher surface temperature. With monthly evapotranspiration averaging 70–100 mm in the dry months (Brando, Paolucci, et al., 2019; Caioni et al., 2020), it is expected that the observed drought-induced reductions in soil moisture could hamper the

functioning of transitional forests, increasing surface temperature (Caioni et al., 2020), especially if combined with increased VPD, which is a critical driver of tree water stress (Novick et al., 2016). In contrast, our results indicated that both the burned plots and the unburned Control maintained ET rates comparable to the average values for the region during drought (Caioni et al., 2020; Lathuillière et al., 2012; Maeda et al., 2017; Silvério et al., 2015). This suggests that burned forests can maintain a high capacity to access and use available soil water and that compounding fire and drought disturbances of fire and drought may not have negative feedbacks on the water cycle.

4.2. Water Absorption in Deep Soil

Disturbances are likely to impact the capacity of trees to uptake deep soil moisture. Nepstad et al. (1994) showed that secondary vegetation exhibits higher seasonality and lower capacity to uptake deep soil moisture compared to primary forests. However, different disturbances may have varying impacts on this capacity. Regarding wildfires, we speculate that fires may impact rooting depth in several ways. First, they can alter the abundance of shallow and deep-rooted trees. Low-intensity wildfires may kill predominantly small-sized trees with shallow roots, while high-intensity fires may kill larger trees with deeper rooting systems. Nevertheless, the relationship between tree size and rooting depth at the species level in tropical forests remains poorly understood, complicating our understanding of how wildfires and recovery affect rooting depth distribution. Second, repeated fires may reduce the time available for the development of deep rooting systems. Third, certain species may have specific water demands. Shallow-rooting trees that colonize burned areas during recovery might consume more shallow water, limiting the recharge of the deep soil profile.

4.3. Implications and Importance of Deep Soil

In our experimental forest, tapping into deep soil moisture helped plants maintain high evapotranspiration during the dry season (Figure 8). Approximately half of the evapotranspiration during the dry season was associated with water uptake deeper than 4 m (Figure S8 in Supporting Information S1). This result is consistent with recent work (Miguez-Macho & Fan, 2021) showing that past precipitation stored in deep soil is the most crucial water source during the dry season in southeastern Amazonia. Although ET declined during drought, the absolute values were still high compared with those in other regions (Figure 8). Maintaining high ET during drought in one of the driest Amazonian forests could help some plants prevent leaf overheating, which is associated with ecologically relevant reductions in photosynthesis. Consistent with observations reported elsewhere in Amazonia (Davidson et al., 2011; Jipp et al., 1998; Nepstad et al., 1994), it is reasonable to assume that trees in our experimental site also accessed soil water below the maximum depth of our sensors. Even so, it is unlikely that all plants at our site could access deep soil water, which could lead to increased water stress in part of the forest community. In addition, the observed differences in soil moisture patterns between the burned and Control plots suggested that postfire vegetation regrowth may deplete soil moisture earlier during droughts than in primary forests.

4.4. Implications of Soil Water Dynamics for the Long-Term Stability of Tropical Forests

Our findings indicate that soil water depletion during drought years may have important implications for other seasonal tropical forests. At our site, the soil provides between 550 and 650 mm of water, which is particularly important supplying water for plants during the dry season. This water supply is sufficient to meet forest water demand in years with normal climatic conditions. However, an extra reduction of >150 mm in soil water during a drought year places forests under considerable water stress, particularly during the dry season following a drought year (Figure 6). This emphasizes the importance of water stored in deep soil for forest maintenance. This is consistent with the results of a rainfall exclusion experiment in the northern Amazon, where the capacity of soil moisture to buffer against vegetation stress (leaf water stress, LAI, and mortality) declined because of long-term reductions in deep soil water storage (Brando et al., 2008; Markewitz et al., 2010; Nepstad et al., 2002, 2007).

Our results indicate that, in the short term, transitional forests can cope with severe droughts such as the ENSO 2015/2016 event. However, this and other studies have pointed out a substantial lag in soil water recharge after an extreme drought (e.g., a year or more; Panday et al., 2015). As droughts become more frequent and intense, the carry-over effect of droughts from one year to the next could cause more severe water stress. Under these conditions, we expect plants to reduce water demand to prevent damage to their vascular systems, given that our experimental forests are growing at the drier end of their climatic limit. It is unclear whether the ENSO of 2015/

2016 caused sufficient vegetation stress to trigger reductions in vegetation growth and the associated carbon fluxes or storage at our site. The forests of southeastern Amazonia are already experiencing increased water stress because of regional climate change, including more frequent and intense droughts (Davidson et al., 2012; Fu et al., 2013). As the region reaches its climatic limit, such changes will almost certainly increase plant water stress. As forests become more stressed, they become more degraded and are likely to emit more carbon than they take up (Gatti et al., 2021).

The rapid depletion of soil moisture in burned forests has two important implications for degraded forest recovery. First, as vegetation recovers, more soil water must be used. This greater use of surface water by recovering vegetation can delay deep soil moisture recharge and extend the dry season. Second, changes in rainfall patterns in the region due to large-scale deforestation (Fu et al., 2013) and the increased frequency of extreme droughts associated with climate change (Duffy et al., 2015) could jeopardize soil moisture recharge and the recovery of these forests, limiting only part of the deep-rooted plant community to access water (Davidson et al., 2011; Nepstad et al., 1994). Together, the interplay between wildfire-induced soil moisture depletion and subsequent recovery of vegetation underscores the critical role of deep soil moisture as a vital water source for forest ecosystems in southeastern Amazonia.

5. Conclusion

The substantial changes in forest dynamics, structure, and composition after our experimental fires were also reflected in the difference in VWC between the Control and annually burned plots (B1yr). However, this result was contrary to our hypothesis, with the burned plots showing lower VWC in the drier months. However, the high fraction of ET from deep groundwater may indicate that our experimental forest is growing close to its climatic safety margin. The ∼150-mm reduction of water in the soil column during the 2015/2016 drought may indicate a future where such extreme events are increasingly common, delaying the recharge of soil moisture in the deep soil. The available soil moisture maintained the transitional forest during an extreme drought, but evidence suggests that ongoing climate changes coupled with deforestation and fires will soon strongly compromise the resilience of these transitional forests.

Conflict of Interest

The authors declare no conflicts of interest relevant to this study.

Data Availability Statement

The soil moisture data from the TDR probes used in this study are available on the DRYAD server: https://datadryad.org/stash/share/m-Bz9PWJPVtLgujc9h809-49D_UNSJixzCIEzpZThY0.

Acknowledgments

We thank the Instituto de Pesquisa Ambiental da Amazônia (IPAM), the Woodwell Climate Research Center (Woodwell), and the Max Planck Institute for Biogeochemistry (MPI-BGC) for providing resources, mentorship, and field support that made this work possible. We thank the outstanding field research team of IPAM for assistance in fieldwork. We also thank the Amaggi Group for enabling access to the experimental area. This work was funded through grants from the Coordination for the Improvement of Higher Education Personnel–Brazil (CAPES/BRASIL; FINANCE CODE 001); The National Science Foundation (IOS 1457602/1457662, DEB 1541851, LTREB 2027827, EAR 1739724, and INFEWS/T1; 2348580); and the National Council for Scientific and Technological Development (CNPq/PELD-TANG; 441703/2016-0 and 441940/2020-0), and National Aeronautics and Space Administration (NASA-80NSSC24K0301), and Bayer. LM was also supported by a São Paulo Research Foundation Grant (FAPESP 2020/06085-1) and L.M.-S. acknowledge the support from the Balzan foundation. DVS was also supported with a productivity grant from CNPq (PQ #311468/2022-5).

References

Alvares, C. A., Stape, J. L., Sentelhas, P. C., de Moraes Gonçalves, J. L., & Sparovek, G. (2013). Köppen's climate classification map for Brazil. *Meteorologische Zeitschrift*, *22*(6), 711–728. https://doi.org/10.1127/0941-2948/2013/0507

Aragǎo, L. E. O. C. (2012). Environmental science: The rainforest's water pump. *Nature*, *489*(7415), 217–218. https://doi.org/10.1038/nature11485

Aragão, L. E. O. C., Anderson, L. O., Fonseca, M. G., Rosan, T. M., Vedovato, L. B., Wagner, F. H., et al. (2018). 21st century drought-related fires counteract the decline of Amazon deforestation carbon emissions. *Nature Communications*, *9*(1), 536. https://doi.org/10.1038/s41467-017-02771-y

Aragão, L. E. O. C., Malhi, Y., Roman-Cuesta, R. M., Saatchi, S., Anderson, L. O., & Shimabukuro, Y. E. (2007). Spatial patterns and fire response of recent Amazonian droughts. *Geophysical Research Letters*, *34*(7). https://doi.org/10.1029/2006GL028946

Balch, J. R. K., Nepstad, D. C., Brando, P. M., Curran, L. M., Portela, O., de Carvalho, O., & Lefebvre, P. (2008). Negative fire feedback in a transitional forest of southeastern Amazonia. *Global Change Biology*, *14*(10), 2276–2287. https://doi.org/10.1111/j.1365-2486.2008.01655.x

Bates, D. M., Bolker, B., & Walker, S. (2015). Fitting linear mixed-effects models using LME4. *Journal of Statistical Software*, *67*(1), 1–48. https://doi.org/10.18637/jss.v067.i01

Brando, P. (2018). Tree height matters. *Nature Geoscience*, *11*(6), 390–391. https://doi.org/10.1038/s41561-018-0147-z

Brando, P. M., Balch, J. K., Nepstad, D. C., Morton, D. C., Putz, F. E., Coe, M. T., et al. (2014). Abrupt increases in Amazonian tree mortality due to drought–fire interactions. *Proceedings of the National Academy of Sciences*, *111*(17), 6347–6352. https://doi.org/10.1073/pnas.1305499111

Brando, P. M., Coe, M. T., DeFries, R., & Azevedo, A. A. (2013). Ecology, economy and management of an agroindustrial Frontier landscape in the southeast Amazon. *Philosophical Transactions of the Royal Society B: Biological Sciences*, *368*(1619), 20120152. https://doi.org/10.1098/rstb.2012.0152

Brando, P. M., Nepstad, D., Davidson, E. A., Trumbore, S. E., Ray, D., & Camargo, P. (2008). Drought effects on litterfall, wood production and belowground carbon cycling in an Amazon forest: Results of a throughfall reduction experiment. *Philosophical Transactions of the Royal Society B*, *363*(1498), 1839–1848. https://doi.org/10.1098/rstb.2007.0031

Brando, P. M., Paolucci, L., Ummenhofer, C. C., Ordway, E. M., Hartmann, H., Cattau, M. E., et al. (2019). Droughts, wildfires, and forest carbon cycling: A pantropical synthesis. *Annual Review of Earth and Planetary Sciences*, *47*(May), 555–581. https://doi.org/10.1146/annurev-earth-082517-010235

Brando, P. M., Silvério, D., Maracahipes-Santos, L., Oliveira-Santos, C., Levick, S. R., Coe, M. T., et al. (2019). Prolonged tropical forest degradation due to compounding disturbances: Implications for CO_2 and H_2O fluxes. *Global Change Biology*, *25*(9), 2855–2868. https://doi.org/10.1111/gcb.14659

Broedel, E., Tomasella, J., Cândido, L. A., & von Randow, C. (2017). Deep soil water dynamics in an undisturbed primary forest in central Amazonia: Differences between normal years and the 2005 drought. *Hydrological Processes*, *31*(9), 1749–1759. https://doi.org/10.1002/hyp.11143

Caioni, C., Silvério, D. V., Macedo, M. N., Coe, M. T., & Brando, P. M. (2020). Droughts amplify differences between the energy balance components of Amazon forests and Croplands. *Remote Sensing*, *12*(3), 525. https://doi.org/10.3390/rs12030525

Coe, M. T., Brando, P. M., Deegan, L. A., Macedo, M. N., Neill, C., & Silvério, D. V. (2017). The forests of the Amazon and Cerrado moderate regional climate and are the key to the future. *Tropical Conservation Science*, *10*(June). https://doi.org/10.1177/1940082917720671

Davidson, E., Lefebvre, P. A., Brando, P. M., Ray, D. M., Trumbore, S. E., Solorzano, L. A., et al. (2011). Carbon inputs and water uptake in deep soils of an eastern Amazon forest. *Forest Science*, *57*(1), 51–58. https://doi.org/10.1093/forestscience/57.1.51

Davidson, E. A., de Araújo, A. C., Artaxo, P., Balch, J. K., Brown, I. F., C. Bustamante, M. M., et al. (2012). The Amazon basin in transition. *Nature*, *481*(7381), 321–328. https://doi.org/10.1038/nature10717

De Faria, B. L., Brando, P. M., Macedo, M. N., Panday, P. K., Soares-Filho, B. S., & Coe, M. T. (2017). Current and future patterns of fire-induced forest degradation in Amazonia. *Environmental Research Letters*, *12*(9), 095005. https://doi.org/10.1088/1748-9326/aa69ce

Duffy, P. B., Brando, P. M., Asner, G. P., & Field, C. B. (2015). Projections of future meteorological drought and wet periods in the Amazon. *Proceedings of the National Academy of Sciences of the United States of America*, *112*(43), 13172–13177. https://doi.org/10.1073/pnas.1421010112

Fu, R., Yin, L., Li, W., Arias, P. A., Dickinson, R. E., Huang, L., et al. (2013). Increased dry-season length over southern Amazonia in recent decades and its implication for future climate projection. *Proceedings of the National Academy of Sciences of the United States of America*, *110*(45), 18110–18115. https://doi.org/10.1073/pnas.1302584110

Gatti, L. V., Basso, L. S., Miller, J. B., Gloor, M., Gatti Domingues, L., Cassol, H. L. G., et al. (2021). Amazonia as a carbon source linked to deforestation and climate change. *Nature*, *595*(7867), 388–393. https://doi.org/10.1038/s41586-021-03629-6

Giardina, F., Konings, A. G., Kennedy, D., Alemohammad, S. H., Oliveira, R. S., Uriarte, M., & Gentine, P. (2018). Tall Amazonian forests are less sensitive to precipitation variability. *Nature Geoscience*, *11*(6), 1–5. https://doi.org/10.1038/s41561-018-0133-5

Guillod, B. P., Orlowsky, B., Miralles, D. G., Teuling, A. J., & Seneviratne, S. I. (2015). Reconciling spatial and temporal soil moisture effects on afternoon rainfall. *Nature Communications*, *6*(1), 6443. https://doi.org/10.1038/ncomms7443

Hayhoe, S., Neil, C., Porder, S., Mchorney, R., Lefbvre, P., Coe, M., et al. (2011). Conversion to soy on the Amazonian agricultural Frontier increases streamflow without affecting stormflow dynamics. *Global Change Biology*, *17*, 1821–1833. https://doi.org/10.1111/j.1365-2486.2011.02392.x

Jipp, P. H., Nepstad, D. C., Cassel, D. K., & Reis De Carvalho, C. (1998). Deep soil moisture storage and transpiration in forests and pastures of seasonally-dry Amazonia. *Climatic Change*, *39*(2), 395–412. https://doi.org/10.1023/A:1005308930871

Lathuillière, M. J., Johnson, M. S., & Donner, S. D. (2012). Water use by terrestrial ecosystems: Temporal variability in rainforest and agricultural contributions to evapotranspiration in Mato Grosso, Brazil. *Environmental Research Letters*, *7*(2), 024024. https://doi.org/10.1088/1748-9326/7/2/024024

Lewis, S. L., Brando, P. M., Phillips, O. L., van der Heijden, G. M. F., & Nepstad, D. (2011). The 2010 Amazon drought. *Science*, *331*(6017), 554. https://doi.org/10.1126/science.1200807

L'Heureux, M. L., Takahashi, K., Watkins, A. B., Barnston, A. G., Becker, E. J., Di Liberto, T. E., et al. (2017). Observing and predicting the 2015/16 El Niño. *Bulletin of the American Meteorological Society*, *98*(7), 1363–1382. https://doi.org/10.1175/BAMS-D-16-0009.1

Lovejoy, T. E., & Nobre, C. (2018). Amazon tipping point. *Science Advances*, *4*(2), 1–2. https://doi.org/10.1126/sciadv.aat2340

Maeda, E. E., Ma, X., Wagner, F., Kim, H., Oki, T., Eamus, D., & Huete, A. (2017). Evapotranspiration seasonality across the Amazon basin. *Earth System Dynamics Discussions*(January), 1–28. https://doi.org/10.5194/esd-2016-75

Malhi, Y., Roberts, J. T., Betts, R. A., Killeen, T. J., Li, W., & Nobre, C. A. (2008). Climate change, deforestation, and the fate of the Amazon. *Science*, *319*(5860), 169–172. https://doi.org/10.1126/science.1146961

Marengo, J. A., & Espinoza, J. C. (2015). Extreme seasonal droughts and floods in Amazonia: Causes, trends and impacts. *International Journal of Climatology*, *36*(3), 1033–1050. https://doi.org/10.1002/joc.4420

Markewitz, D., Devine, S., Davidson, E. A., Brando, P., & Nepstad, D. C. (2010). Soil moisture depletion under simulated drought in the Amazon: Impacts on deep root uptake. *New Phytologist*, *187*(3), 592–607. https://doi.org/10.1111/j.1469-8137.2010.03391.x

McDowell, N. G., Allen, C. D., Anderson-Teixeira, K., Aukema, B. H., Bond-Lamberty, B., Chini, L., et al. (2020). Pervasive shifts in forest dynamics in a changing world. *Science*, *368*(6494). https://doi.org/10.1126/science.aaz9463

Miguez-Macho, G., & Fan, Y. (2021). Spatiotemporal origin of soil water taken up by vegetation. *Nature*, *598*(7882), 624–628. https://doi.org/10.1038/s41586-021-03958-6

Miller, S. D., Goulden, M. L., Hutyra, L. R., Keller, M., Saleska, S. R., Wofsy, S. C., et al. (2011). Reduced impact logging minimally alters tropical rainforest carbon and energy exchange. *Proceedings of the National Academy of Sciences*, *108*(48), 19431–19435. https://doi.org/10.1073/pnas.1105068108

Morton, D. C., Le Page, Y., DeFries, R., Collatz, G. J., & Hurtt, G. C. (2013). Understorey fire frequency and the fate of burned forests in southern Amazonia. *Philosophical Transactions of the Royal Society B: Biological Sciences*, *368*(1619), 20120163. https://doi.org/10.1098/rstb.2012.0163

Nagy, R. C., Porder, S., Neill, C., Brando, P., Quintino, R. M., & Do Nascimento, S. A. (2015). Structure and composition of altered riparian forests in an agricultural Amazonian landscape. *Ecological Applications*, *25*(6), 1725–1738. https://doi.org/10.1890/14-1740.1

Nepstad, D. C., de Carvalho, C. R., Davidson, E. A., Jipp, P. H., Lefebvre, P. A., Negreiros, G. H., et al. (1994). The role of deep roots in the hydrological and carbon cycles of Amazonian forests and pastures. *Nature*, *372*(6507), 666–669. https://doi.org/10.1038/372666a0

Nepstad, D. C., Moutinho, P., Dias-Filho, M. B., Davidson, E., Cardinot, G., Markewitz, D., et al. (2002). The effects of partial throughfall exclusion on canopy processes, aboveground production, and biogeochemistry of an Amazon forest. *Journal of Geophysical Research*, *107*(D20). https://doi.org/10.1029/2001JD000360

Nepstad, D. C., Tohver, I. M., David, R., Moutinho, P., & Cardinot, G. (2007). Mortality of large trees and lianas following experimental drought in an Amazon forest. *Ecology*, *88*(9), 2259–2269. https://doi.org/10.1890/06-1046.1

Nobre, C., Sampaio, G., Borma, L., Cardoso, M., Castilla-Rubio, J., & Silva, J. (2016). Land-use and climate change risks in the Amazon and the need of a novel sustainable development paradigm. *Proceedings of the National Academy of Sciences of the United States of America*, *113*(39), 10759–10768. https://doi.org/10.1073/pnas.1605516113

Novick, K. A., Ficklin, D. L., Stoy, P. C., Williams, C. A., Bohrer, G., Oishi, A. C., et al. (2016). The increasing importance of atmospheric demand for ecosystem water and carbon fluxes. *Nature Climate Change*, *6*(11), 1023–1027. https://doi.org/10.1038/nclimate3114

Panday, P. K., Coe, M. T., Macedo, M. N., Lefebvre, P., & Castanho, A. D. D. A. (2015). Deforestation offsets water balance changes due to climate variability in the Xingu River in eastern Amazonia. *Journal of Hydrology*, *523*, 822–829. https://doi.org/10.1016/j.jhydrol.2015.02.018

Pfautsch, S. (2016). Hydraulic anatomy and function of trees—Basics and critical developments. *Current Forestry Reports*, *2*(4), 236–248. https://doi.org/10.1007/s40725-016-0046-8

Phillips, O. L., Aragão, L. E. O. C., Lewis, S. L., Fisher, J. B., Lloyd, J., López-gonzález, G., et al. (2009). Drought sensitivity of the Amazon rainforest, *323*(March), 1344–1347.

Pittermann, J. (2010). The evolution of water transport in plants: An integrated approach. *Geobiology*, *8*(2), 112–139. https://doi.org/10.1111/j.1472-4669.2010.00232.x

R Core Team. (2023). *R: A language and environment for statistical computing*. R Foundation for Statistical Computing. Retrieved from https://www.R-project.org/

Rocha, W., Metcalfe, D. B., Doughty, C. E., Brando, P., Silvério, D., Halladay, K., et al. (2014). Ecosystem productivity and carbon cycling in intact and annually burnt forest at the dry southern limit of the Amazon rainforest (Mato Grosso, Brazil). *Plant Ecology & Diversity*, *7*(1–2), 25–40. https://doi.org/10.1080/17550874.2013.798368

Salati, E., Dall'Olio, A., Matsui, E., & Gat, J. R. (1979). Recycling of water in the Amazon Basin: An isotopic study. *Water Resources Research*, *15*(5), 1250–1258. https://doi.org/10.1029/WR015i005p01250

Scheffler, R., Neill, C., Krusche, A. V., & Elsenbeer, H. (2011). Soil hydraulic response to land-use change associated with the recent soybean expansion at the Amazon agricultural Frontier. *Agriculture, Ecosystems & Environment*, *144*(1), 281–289. https://doi.org/10.1016/j.agee.2011.08.016

Silveiro, A. C., Silvério, D. V., Macedo, M. N., Coe, M. T., Maracahipes, L., Uribe, M., et al. (2024). Tanguro field station - Time Domain Reflectometry (TDR) dataset [Dataset]. *Dryad*. https://doi.org/10.5061/dryad.d51c5b09w

Silvério, D. V., Brando, P. M., Macedo, M. N., Beck, P. S. A., Bustamante, M., & Coe, M. T. (2015). Agricultural expansion dominates climate changes in southeastern Amazonia: The overlooked non-GHG forcing. *Environmental Research Letters*, *10*(10), 104015. https://doi.org/10.1088/1748-9326/10/10/104015

Solander, K. C., Newman, B. D., Carioca De Araujo, A., Barnard, H. R., Berry, Z. C., Bonal, D., et al. (2020). The pantropical response of soil moisture to El Niño. *Hydrology and Earth System Sciences*, *24*(5), 2303–2322. https://doi.org/10.5194/hess-24-2303-2020

Spanner, G. C., Gimenez, B. O., Wright, C. L., Menezes, V. S., Newman, B. D., Collins, A. D., et al. (2022). Dry season transpiration and soil water dynamics in the central Amazon. *Frontiers in Plant Science*, *13*. https://doi.org/10.3389/fpls.2022.825097

Spracklen, D. V., Arnold, S. R., & Taylor, C. M. (2012). Observations of increased tropical rainfall preceded by air passage over forests. *Nature*, *489*(7415), 282–285. https://doi.org/10.1038/nature11390

Staal, A., VanNes, E., Scheffer, M., Tuinenburg, O., Dekker, S., Bosmans, J., et al. (2018). Forest-rainfall cascades buffer against drought across the Amazon. *Nature Climate Change*, *8*(6), 539–543. https://doi.org/10.1038/s41558-018-0177-y

Sungmin, O., XinyuanOrth, H. R., & Rene, O. (2020). Observational evidence of wildfire-promoting soil moisture anomalies. *Scientific Reports*, *10*(1), 11008. https://doi.org/10.1038/s41598-020-67530-4

Topp, G. C., Davis, J. L., & Annan, A. P. (1980). Electromagnetic determination of soil water content: Measurements in coaxial transmission lines. *Water Resources Research*, *16*(3), 574–582. https://doi.org/10.1029/WR016i003p00574

Trenberth, K. E. (1997). The definition of El Niño. *Bulletin of the American Meteorological Society*, *78*(12), 2771–2777. https://doi.org/10.1175/1520-0477(1997)078<2771:TDOENO>2.0.CO;2

Wright, J. S., Fu, R., Worden, J. R., Chakraborty, S., Clinton, N. E., Risi, C., et al. (2017). Rainforest-initiated wet season onset over the southern Amazon. *Proceedings of the National Academy of Sciences of the United States of America*, *114*(32), 8481–8486. https://doi.org/10.1073/pnas.1621516114

Yang, Y., Saatchi, S. S., Xu, L., Yu, Y., Choi, S., Phillips, N., et al. (2018). Post-drought decline of the Amazon carbon sink. *Nature Communications*, *9*(1), 3172. https://doi.org/10.1038/s41467-018-05668-6